Inorganic Chemistry

Article

pubs.acs.org/IC

Effect of Cobalt Substitution on $Li_{3-2x}Co_xN$ Local Structure: A XAS Investigation

Diane Muller-Bouvet,*[,†,‡] Jean-Pierre Pereira-Ramos,[†,‡] Stéphane Bach,[†,‡,§] Patrick Willmann,[∥] and Alain Michalowicz[‡]

[†]GESMAT and [‡]Institut de Chimie et des Matériaux Paris Est, UMR CNRS UPEC 7182, 2 rue Henri Dunant, 94320 Thiais, France

[§]Université d'Evry Val d'Essonne, Département Chimie, Bd F. Mitterrand, 91025 Evry Cedex, France

[∥]CNES, 118 avenue Edouard Belin, 31401 Toulouse Cedex 9, France

ABSTRACT: The influence of cobalt substitution on the local structural changes around Co atoms in the layered lithium nitridocobaltates $Li_{3-2x}Co_xN$ for $0.05 \leq x \leq 0.44$ is investigated using Co K-edge X-ray absorption spectroscopy (EXAFS and XANES). The Co−N bond length in $Li_{3-2x}Co_xN$ compounds is obtained vs x by performing EXAFS fitting and found to be shorter (1.80 Å) than for $x = 0$ (Li_3N), and its value does not change with x. A comparison of EXAFS data with XRD results is discussed. We show that the continuous decrease of interlayer distance versus Co content (x), described from XRD data, accounts for an average of the Co−N and Li−N distances, weighted by the number of these bond lengths. In addition, the present work supports the proposal that the Li_{1b}−N bonds contract with x due to a significant increase of Coulombic attractive forces locally induced by the progressive Li^+/Co^{2+} substitution. XRD studies suggested that divalent Co ions bond to two nitrogen in $Li_{3-2x}Co_xN$. Although additional works are still needed to prove its valence, the present XAFS findings complements the local structure found by XRD, in good accord with the electrochemical properties previously reported.

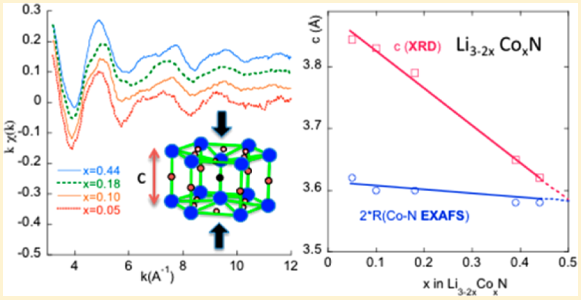

INTRODUCTION

Layered lithium transition metal nitrides have been studied in the pioneering work of Shodai et al. and Nishijima et al. as alternative anode materials for rechargeable Li batteries.[1−4] Among them, $Li_{2.6}Co_{0.4}N$ has been selected due to its high specific capacity and cycle performance in the 1.4/0 V potential window. In addition, many efforts have been made to optimize its cycling behavior by using composite anode systems containing $Li_{2.6}Co_{0.4}N$ and hard carbon, metallic oxide powders, or alloys.[5−7] More recently our group has reported a detailed investigation of the lithium cobalt nitrides $Li_{3-2x}Co_xN$ ($0.1 \leq x \leq 0.44$) in the 1/0.02 V potential window and demonstrated their interest as genuine Li intercalation compounds with an excellent cycle life.[8,9] This remarkable cycling stability is explained by the lack of structural changes indicating a probable reversible Li insertion in lithium vacancies of the pristine lithiated nitridocobaltate. A maximum Co content of about 0.4 was also chosen for its high capacity (200 mAh g^{-1}). The $Li_{3-2x}Co_xN$ compounds are layered host lattices derived from the Li_3N structure. Electrochemical and structural data from refs 8 and 9 indicate that the substituent cobalt ions, in place of interlayer Li ions, can be considered in a divalent state with the correlative presence of the same amount of Li vacancies located in the nitride plane.[8−10] Similar results have been obtained with nitridonickelates.[11] More precisely, an XRD study of $Li_{3-2x}Co_xN$ revealed a linear decrease of the cell volume versus Co content showing a solid solution behavior of the $Li_{3-2x}Co_xN$ system for $0.1 \leq x \leq 0.44$. The hexagonal symmetry of Li_3N was maintained without any change in terms of ordering in spite of the high value of Li/Co substitution. In order to better understand the consequence of Li substitution by Co ions on the layered ordered structure of Li_3N, an EXAFS study is required to investigate the Co local structure. The first and sole EXAFS study on transition metal−lithium nitrides has been reported on only one composition ($Li_{2.6}Co_{0.4}N$)[10] and as a function of the depth of charge and discharge. In this paper, the authors showed that the local structure around Co ions was not significantly affected by the first electrochemical Li extraction−insertion cycle, but no data were reported as a function of cobalt content. Therefore, we decided to examine the influence of Co content on the local structural changes in the lithium cobalt nitrides group $Li_{3-2x}Co_xN$ ($0.1 \leq x \leq 0.44$) using the EXAFS technique.

CHEMICAL SYNTHESIS

The lithium cobalt nitride compounds were prepared using a solid state route from the reagent grade Li_3N (Alfa-Aesar 99.5%, 10 μm; $P6/mmm$, $a = b = 3648$ Å, $c = 3875$ Å[12]) and Co metal (Alfa-Aesar 99.8%, 1.6 μm). To obtain $Li_{3-2x}Co_xN$ with different x values, a mixture of Li_3N and Co in a ratio R (R = Co/Li_3N) was first mixed and ground in agate mortar and then pressed to get a pellet 1 cm in diameter and 5−8 mm in thickness. The pellet of about 1 g is then transferred on a

Received: March 7, 2014
Published: June 4, 2014

   dx.doi.org/10.1021/ic500528f | *Inorg. Chem.* 2014, 53, 6127−6131

tungsten foil in an alumina crucible and heat-treated at the desired temperature at 700 °C for 8 h in a nitrogen gas stream. The oven is first at 300 °C, and a heating rate of 50 °C h^{-1} is used to reach 700 °C. The chemical composition of the compounds was determined by elemental analysis (inductively coupled plasma−atomic emission spectroscopy: ICP-AES) with an accuracy of ±2%. Handling and storage were performed under an argon atmosphere.

XAS MEASUREMENTS AND ANALYSIS

X-ray absorption spectra are treated and analyzed with MAX, a suite of XAFS data analysis programs.[13] The quantities of nitrides were calculated in order to obtain a total absorbance after the edge $\mu x(E) < 2$ with MAX-Absorbix. Spectra were recorded in transmission mode at Soleil (the French synchrotron radiation facility), with the following experimental conditions: K Co edge, energy range 7650−7830 eV. Spectra were recorded on the SAMBA station, with a Si (2 2 0) monochromator and a focusing−harmonic rejection mirror. The XANES and EXAFS spectra were extracted using the standard procedures[14−16] available in MAX-Cherokee, including spline smoothing atomic absorption determination, energy dependent normalization, and Fast Fourier Transform (E_0 = 7718 eV, FT range: 2−12 Å^{-1}) and Fourier filtering of the first peak. Each spectrum was recorded three times and averaged. FEFF8[17] input files were prepared with the code CRYSTALFF,[18] using the knowledge of lithium cobalt nitrides structure.[8] Fits are performed with Round Midnight code[13] by comparing the experimental spectra to the EXAFS standard formula [equation1].

$$k\chi(k) = -S_0^2 \sum_i \frac{N_i}{R_i^2} |f_i(k, R_i)|\, e^{-2\sigma_i^2 k^2}\, e^{-2R_i/\lambda(k)} \sin[2kR_i + 2\delta_1(k) + \psi_i(k)] \quad (1)$$

S_0^2 is the amplitude reduction factor; N_i is the number of equivalent scattering paths with an effective distance R_i. $\lambda(k)$ is the mean-free path of the photoelectron. σ_i is the Debye−Waller coefficient, characteristic of the distance distribution width for path i. $\delta_1(k)$ is the central atom phase shift, $|f_i(k)|$ and $\psi_i(k)$ are the amplitude and phase for the neighbor scattering factors, calculated by FEFF8 code. Since theoretical phase shifts and amplitudes were used, it is necessary to fit the energy threshold E_0. The photoelectron mean free path is set to the empirical formula [eq 2]:

$$\lambda(k) = \frac{1}{\Gamma}\left[k + \left(\frac{\eta}{k}\right)^4\right] \quad (2)$$

Values for Γ and η are set to the standard values: η = 3.0 and Γ = 1. In this modeling of the filtered first coordination sphere, we have fitted a Debye−Waller (DW) factor σ_i and a ΔE_0.

The goodness of fit, or quality factor, is QF = $\Delta\chi_{min}{}^2/\nu$ where $\Delta\chi_{min}$ is the minimum value of the statistical $\Delta\chi_{stat}{}^2$ [eq 3], and the degree of freedom $\nu = N_{ind} - N_{par}$. N_{ind} is the number of independent points $N_{ind} = 2\Delta k\Delta R/\pi$ and N_{par}, the total number of fitted parameters.

$$\Delta\chi_{stat}^2 = \frac{N_{ind}}{N_{pt}} \sum_i \frac{[k\chi_{th}(i) - k\chi_{exp}(i)]^2}{\varepsilon_i^2} \quad (3)$$

In eq 3, N_{pt} is the number of experimental points, and ε_i^2 is the experimental error.

Statistical errors on the average spectra and error bars of the fitted parameters are evaluated as recommended by the IXS Standard and Criteria subcommittee.[19]

The EXAFS spectra are fitted in the range 3−12 Å^{-1}. R-space fitted range is 1−2 Å for the first shell fits. Number of independent points is 6. The average experimental error is evaluated to $\langle\varepsilon\rangle$ = 0.010.

RESULTS AND DISCUSSION

The normalized XANES spectra of $Li_{3-2x}Co_xN$ at the cobalt K edge with x = 0.05, 0.10, 0.18, and 0.44, compared to the cobalt metal foil one, are presented in Figure 1. For the three first Co concentrations, the presence of metallic Co can be completely discarded, whereas it is suspected for x = 0.44.

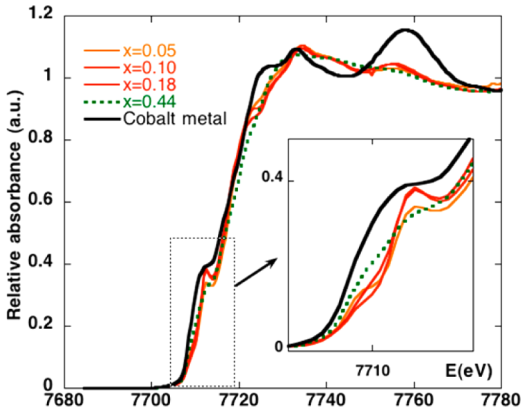

Figure 1. XANES spectra of Co metal foil, and $Li_{3-2x}Co_xN$ for x = 0.05, 0.10, 0.18, and 0.44.

The main features of the $Li_{3-2x}Co_xN$ XANES spectra at the cobalt K edge, in the pre-edge, and edge regions are at 1.5 eV higher energy than for the metal foil for x = 0.05 to 0.18. For x = 0.44, the pre-edge shoulder position is intermediate between those of metallic cobalt and the three lower concentrations. This behavior confirms our suspicion of a small amount of metallic cobalt in this sample. For x = 0.05 to 0.18, the 1.5 eV energy shift indicates that the cobalt atom in $Li_{3-2x}Co_xN$ is oxidized compared to the neutral metal atom. Unfortunately, in the absence of a model compound with a known atomic and electronic structure, we are unable to use these pre-edge feature positions in energy as a direct and reliable measurement of the actual cobalt ionization state. Indeed, edge structures are sensitive both to the local atomic structure and to the electronic state of the absorbing atom. Moreover, *ab initio* XAFS codes (FEFF or FDMNES[20]) at the transition metal K edges are more sensitive to the structure than to the valence and are unable to give edge features absolute energy positions. This is why the 1.5 eV shift for $Li_{3-2x}Co_xN$ samples compared to the pre-edge energy position of the zerovalent metal is a good indication, but not sufficient to prove definitely that the cobalt ion is charged +2, as expected from the emergence of Li vacancies suggested by electrochemical and powder XRD study (Table 1).[8] To use the XANES part of the spectra as a cobalt electronic state probe, *in situ* XAFS experiments under controlled current are planned.

The EXAFS spectra of four lithium cobalt nitrides $Li_{3-2x}Co_xN$ (for x = 0.05 0.10, 0.18, and 0.44) are presented in Figure 2a and the modulus of their Fourier transforms in Figure 2b. The Fourier transforms present two main peaks

dx.doi.org/10.1021/ic500528f | Inorg. Chem. 2014, 53, 6127−6131

Table 1. Wyckoff Positions for $Li_{3-2x}Co_xN$ (*P6/mmm* space group)[21] and Crystal Structure of $Li_{3-2x}Co_xN$ Compounds

ion	Wyckoff position	x	y	z	occupancy	calculated distances to Co in $Li_{2.79}Co_{0.1}N$ (Å) from ref 21
N^{3-}	1a	0	0	0	1	1.91
Li^+ (2)	2c	2/3	1/3	0	$1 - x/2$	2.85
Li^+ (1)	1b	0	0	1/2	$1 - x$	3.66
Co^{2+}	1b	0	0	1/2	x	

pointing at 1.4 and 2.1 Å. The first peak position is independent of the cobalt concentration x, while its intensity is slightly modified. On the contrary, we observe a significant variation of the second peak height versus x. For x = 0.05, 0.10, and 0.18, the amplitude of this peak decreases with Co content. The case of x = 0.44 is particular since an important increase of its height is observed. Traces of metallic Co cannot be discarded to explain the unexpected amplitude of this peak. Indeed, the $Li_{2.12}Co_{0.44}N$ composition corresponds to the maximum solubility of Co in Li_3N solid solution.[8] The position of the second peak is the same for x = 0.10, 0.18, and 0.44 and slightly higher for x = 0.05. This small shift is not in disagreement with the structural changes observed by XRD,[8] i.e., a coevolution of the parameters a and c, which generates a decrease of Co−Li(1b) distance with cobalt substitution.

The $Li_{2.23}Co_{0.39}N$ spectrum is not presented because it appeared to be a mixture of lithium cobalt nitride and a significant amount of metallic cobalt. This is probably due to the fact that the Co concentration is close to the solubility limit.[8] In this case, the complex EXAFS signal beyond the first coordination sphere discussed above is also mixed with a metallic cobalt−cobalt contribution at 2.49 Å. This is why we have focused our quantitative analysis on the first filtered coordination sphere, which is sufficiently separated from the farther contributions.

In order to analyze the Fourier transform pattern, we have performed a FEFF[17] *ab initio* simulation, based on the powder crystal structure for $0.05 \leq x \leq 0.44$.[8,21] The use of the Max-Crystalffrev program facilitates the theoretical FEFF study of such disordered materials. In our case, there are two different sources of disorder: (i) partial substitution of Li by Co in the 1b site and (ii) apparition of Li vacancies in the 2c site. Both Co ions and Li vacancies are randomly distributed, and Crystalffrev is able to take these random distributions into account in the FEFF input file.

The first peak at 1.4 Å (Figure 2b) is clearly identified as the first neighbor Co−N signal, corresponding to the cobalt and nitrogen atoms lying respectively in 1b and 1a sites, on the c axis (Table 1 and Figure 3).

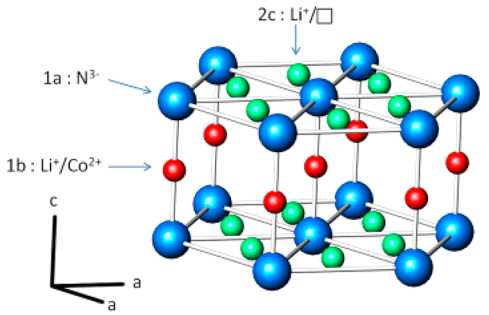

Figure 3. Crystal structure of $Li_{3-2x}Co_xN$ compound. Nitrogen ions are in the 1a site, lithium ions in 1b and 2c sites, and cobalt ions in the 1b site.[22]

Beyond the first coordination sphere, the photoelectron paths analysis is more complicated, with a mixing of single Co−Li_{2c} scattering path and multiple scattering paths implying nitrogen and lithium (1b). However, despite these EXAFS signals being affected by an important disorder due to partial substitution and vacancies, the second peak at 2.1 Å can be assigned essentially to lithium ions in 2c sites. This assumption is supported by the decreasing intensity with Co content (Figure 2b): the higher the Co content, the higher the Li vacancies in 2c sites, and the lower the peak intensity.

The fit results for the first Co−N EXAFS signal are summarized in Table 2 and Figure 4 (x = 0.10 taken as example). The Debye−Waller factor σ^2 and bond length R_{Co-N} were fitted. The goodness of fit was estimated using the quality factor QF. The high value of QF for $Li_{2.9}Co_{0.05}N$ can be

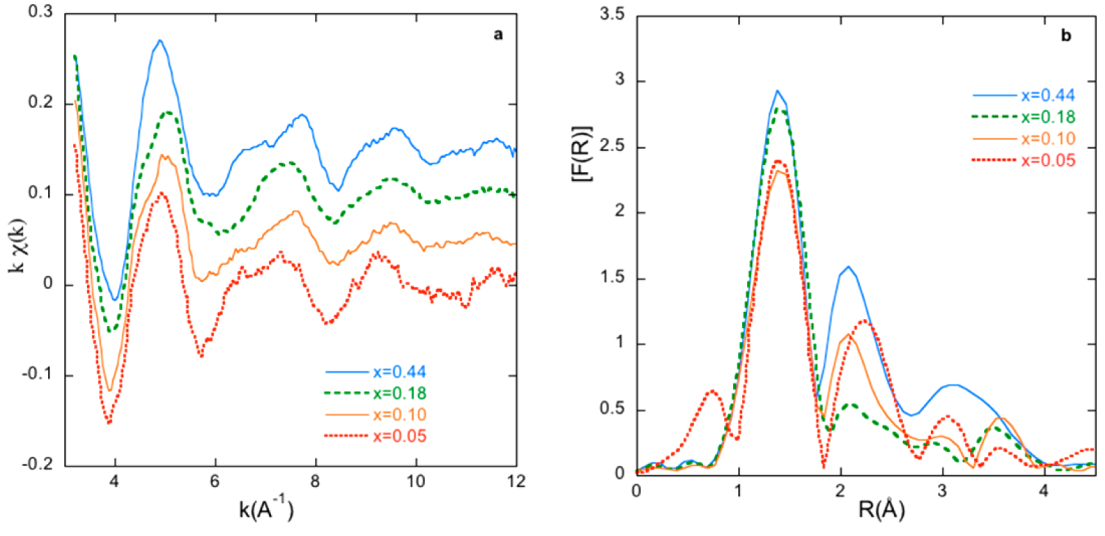

Figure 2. Comparison of EXAFS spectra of the lithium cobalt nitrides $Li_{3-2x}Co_xN$ and their Fourier Transform modulus.

dx.doi.org/10.1021/ic500528f | Inorg. Chem. 2014, 53, 6127−6131

Table 2. Fit Parameters of the First Coordination Shell for Lithium Cobalt Nitrides $Li_{3-2x}Co_xN$

	R_{Co-N} (Å)	σ^2 (Å^2) × 10^3	QF	c/2 (Å) XRD[8]
$Li_{2.90}$ $Co_{0.05}$ N	1.81 (1)	2 (1)	2.9	1.92[a]
$Li_{2.79}$ $Co_{0.10}$ N	1.80 (1)	4.7 (1)	0.37	1.91
$Li_{2.64}Co_{0.18}N$	1.80 (1)	3.5 (9)	0.64	1.89
$Li_{2.23}Co_{0.39}N$	1.79 (3)	6 (1)	1.25	1.82
$Li_{2.12}Co_{0.44}N$	1.79 (1)	2.8 (6)	0.38	1.81

[a]Value obtained by interpolation between $x = 0$ and $x = 0.10$.

explained by the very low amount of absorbing cobalt atoms in the sample. The EXAFS fitted distances are compared with $c/2$, the Co−N distance obtained by XRD.[8] It is worth noticing that the EXAFS refined distances are between 1.79 and 1.81, regardless of the cobalt composition. This result is coherent with the EXAFS fitting of $Li_{2.6}Co_{0.44}N$ in ref 10. The error bar for R_{Co-N} in $Li_{2.23}Co_{0.39}N$ is larger than for the other compositions, since this sample is polluted by a large amount of metallic cobalt, and the filtering of the first Co−N contribution is affected by more systematic errors. Hence, it appears that the local Co−N distance probed by EXAFS is constant within the error bars. On the contrary, distances obtained by XRD showed a linear decrease with x value (Figure 5).

For lithium cobalt nitrides, the cobalt−nitrogen distance (1.80 Å) obtained in this work is shorter than the lithium−nitrogen distance found in the Li_3N crystal structure (1.937 Å).[12] These apparent contradictory results can be explained. Indeed, our EXAFS results prove that the $c/2$ value (interlayer spacing) determined by XRD is actually the average of the Li−N and Co−N distances, respectively weighted by the number of these distances: $1 - x$ and x. In other respects, as shown in Figure 5, c(XRD) decreases more rapidly versus x than simply expected for an average Vegard's law,[23] in which the two extreme distances, for Li−N and Co−N, are assumed to be constant. If this law was strictly followed, c(XRD) should be equal to c(EXAFS) for $x = 1$, and not for $x = 0.5$, as suggested in Figure 5. The interlayer distance found from XRD decreases more rapidly than expected from the number of Co−N bonds. Thus, it seems that, unlike the Co−N distance, the Li_{1b}−N

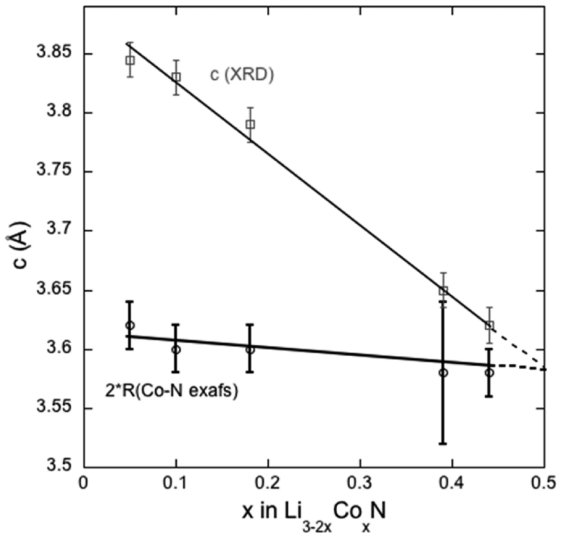

Figure 5. Evolution of the unit cell parameter c (□) and the interlayer spacing ($c = 2*d_{Co-N}$) obtained from EXAFS modeling (○), as a function of x in $Li_{3-2x}Co_xN$.

distance decreases significantly with x. It can be suggested that the Li_{1b}−N bond length, close to Co_{1b}−N, is also shortened, due to the strong Coulombic attractive forces locally induced by the progressive Li_{1b}^+/Co_{1b}^{2+} substitution. Since the Co substitution is disordered, the resulting decrease of the Li−N bond length induces important local distortions in the structure, which are averaged in the XRD refinement. The second peak height reduction with Co content observed in Figure 2b for $x = 0.05$ to $x = 0.18$ confirms this assumption. Indeed, substitution of Li^+ by Co^{2+} in 1b sites leads to vacancies in 2c sites, and then to a decrease of the number of neighbor Li^+.

The apparent mismatch between XRD results and the EXAFS data present in this work is not a unique example of such a substitution disorder and crystallographic average effect. On the contrary, it is largely expected in such solid solutions. Powder or even monocrystal diffraction studies of partially substituted disordered materials can lead to a correct average of the long-range order structures but only approximate local

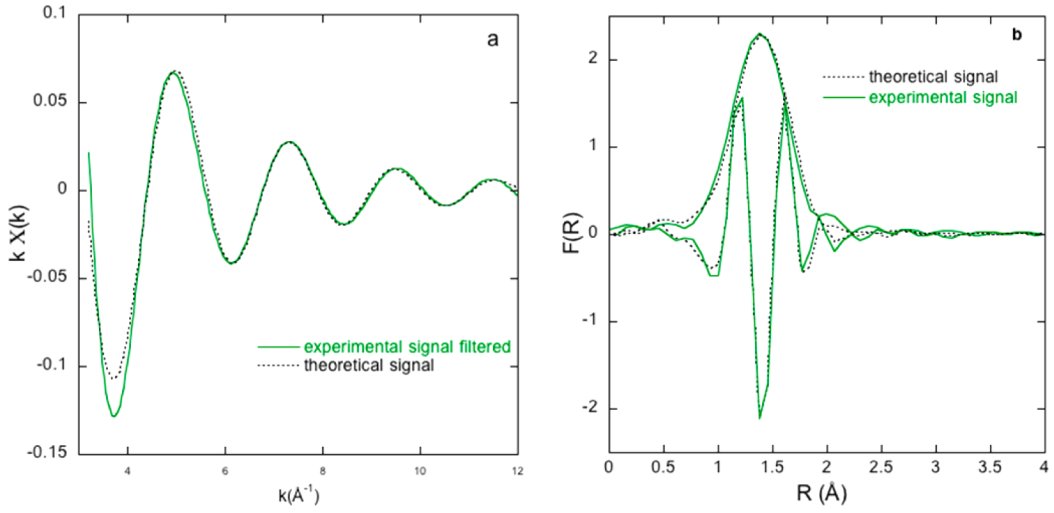

Figure 4. Comparison between experimental and theoretical signals for $Li_{2.12}Co_{0.10}N$. (a) EXAFS spectrum and (b) corresponding Fourier transform.

dx.doi.org/10.1021/ic500528f | Inorg. Chem. 2014, 53, 6127−6131

structures. This disorder effect on the diffraction patterns is fully described in Guinier's textbook.[24] It has been confirmed by the complementary diffraction and EXAFS studies of various materials such as metallic alloys,[25,26] metallic oxides,[27−29] and lamellar compounds.[30,31] As in our case, all these materials are solid solutions. Their XRD refinements lead to linear variations of crystal lattices versus composition. In this work, and all the papers cited above, the local interatomic distance around the absorbing atom probed by EXAFS remains almost constant versus substitute composition, and the linear variations of the crystal parameters are due to a substitution disorder average effect.

CONCLUSION

In summary, the main results found in the present XAFS study of $Li_{3-2x}Co_xN$ for $0.05 \leq x \leq 0.44$ show that Co atoms are oxidized compared to metallic Co. Moreover the cobalt second neighbor behavior (peak amplitude decreases with Co content) confirms the formation of Li vacancies in 2c sites with x, which indicates that Co is probably divalent. The solid solution nature of $Li_{3-2x}Co_xN$ with x is confirmed. The average linear decrease of the interlayer spacing found from XRD can be clarified by two main EXAFS findings. First, the Co_{1b}−N distance (1.80 Å) is shorter than the Li_{1b}−N bond (1.937 Å) in Li_3N and constant regardless of x value. It is the driving force to explain the c parameter decrease with x. Second this result reveals that the Li_{1b}−N bonds also are affected and decrease with x. The latter phenomenon reflects the regular increase of Coulombic attractive forces locally induced by the progressive Li^+/Co^{2+} substitution in 1b sites. These two effects are combined to account for the XRD data on interlayer evolution with x in $Li_{3-2x}Co_xN$.

AUTHOR INFORMATION

Corresponding Author

*E-mail: muller@u-pec.fr.

Notes

The authors declare no competing financial interest.

ACKNOWLEDGMENTS

The authors would like to thank the Samba beamline staff (synchrotron Soleil) and the members of SAX group (ICMPE) for technical support and helpful discussions.

REFERENCES

(1) Shodai, T.; Okada, S.; Tobishima, S.-i.; Yamaki, J.-i. *Solid State Ionics* **1996**, *86−88*, 785−789.
(2) Shodai, T.; Okada, S.; Tobishima, S.; Yamaki, J. *J. Power Sources* **1997**, *68*, 515−518.
(3) Nishijima, M.; Kagohashi, T.; Takeda, Y.; Imanishi, M.; Yamamoto, O. *J. Power Sources* **1997**, *68*, 510−514.
(4) Nishijima, M.; Kagohashi, T.; Imanishi, M.; Takeda, Y.; Yamamoto, O.; Kondo, S. *Solid State Ionics* **1996**, *83*, 107−111.
(5) Sun, H.; He, X.; Li, J.; Ren, J.; Jiang, C. Y.; Wan, C. *Solid State Ionics* **2006**, *177*, 1331−1334.
(6) Yang, J.; Takeda, Y.; Li, Q.; Imanishi, N.; Yamamoto, O. *J. Power Sources* **2001**, *97−98*, 779−781.
(7) Yang, J.; Takeda, Y.; Imanishi, N.; Yamamoto, O. *Electrochim. Acta* **2001**, *46*, 2659−2664.
(8) Ducros, J.-B.; Bach, S.; Ramos, J.-P. P.; Willmann, P. *J. Power Sources* **2008**, *175*, 517−525.
(9) Ducros, J. B.; Bach, S.; Pereira-Ramos, J. P.; Willmann, P. *Electrochem. Commun.* **2007**, *9*, 2496−2500.
(10) Kim, T. Y.; Kim, M. G.; Lee, J. M.; Kang, T.; Sohn, H.-J. *Electrochem. Solid-State Lett.* **2002**, *5*, A103−A106.
(11) Ducros, J. B.; Bach, S.; Pereira-Ramos, J. P.; Willmann, P. *Electrochim. Acta* **2007**, *52*, 7035−7041.
(12) Rabenau, A.; Schulz, H. *J. Less-Common Met.* **1976**, *50*, 155−159.
(13) Michalowicz, A.; Moscovici, J.; Muller-Bouvet, D.; Provost, K. *J. Phys.: Conf. Ser.* **2009**, 012034.
(14) Teo, B. K. *EXAFS: Basic Principles and Data Analysis*; Springer-Verlag: New York, 1986; Vol. *103*.
(15) Koenigsberger, D. C.; Prins, R. In *X-Ray Absorption Principles, Applications, Techniques of EXAFS, SEXAFS and XANES*; John Wiley: New York, 1988.
(16) Bunker, G. *Introduction to XAFS, a practical guide to X-ray absorption fine structure spectroscopy*; Cambridge University Press: Cambridge, U.K., 2010.
(17) Ankudinov, A. L.; Ravel, B.; Rehr, J. J.; Conradson, S. D. *Phys. Rev. B* **1998**, *58*, 7565−7576.
(18) Provost, K.; Champloy, F.; Michalowicz, A. *J. Synchrotron Radiat.* **2001**, *8*, 1109−1112.
(19) Sayers, D. E. Report of the International XAFS Society Standards and Criteria Commitee. http://ixs.iit.edu/subcommittee_reports/sc/ (accessed May 16, 2014).
(20) Bunau, O.; Joly, Y. *J. Phys.: Condens. Matter* **2009**, *21*, 345501.
(21) Ducros, J.-B. Synthese et etude electrochimique de nitrures mixtes de lithium et de métal de type $Li_{3-x}M_xN$ (M=Co, Cu, Ni) utilisables comme électrode négative dans les accumulateurs Li-ion. Ph.D. Thesis, Université Paris XII, France, 12 Décembre 2006.
(22) Panabiere, E.; Emery, N.; Bach, S.; Pereira-Ramos, J.-P.; Willmann, P. *Corros. Sci.* **2012**, *58*, 237−241.
(23) Vegard, L. *Z. Phys.* **1921**, *5*, 17−26.
(24) Guinier, A. *X-Ray Diffraction in crystals, Imperfect Crystals, and Amorphous Bodies*; Dover: New York, 1994.
(25) Mimault, J.; Fontaine, A.; Lagarde, P.; Raoux, D.; Sadoc, A.; Spanjaard, D. *J. Phys. F* **1981**, *11*, 1311−1326.
(26) Sadoc, A.; Calvayrac, Y.; Quivy, A.; Harmelin, M.; Flank, A. M. *J. Non-Cryst. Solids* **1984**, *65*, 109−129.
(27) Kuzmin, A.; Mironova, N. *J. Phys.: Condens. Matter* **1998**, *10*, 7937−7944.
(28) Moscovici, J.; Rougier, A.; Laruelle, S.; Michalowicz, A. *J. Chem. Phys.* **2006**, *125*, 124505.
(29) Tarantino, S. C.; Ghigna, P.; McCammon, C.; Amantea, R.; Carpenter, M. A. *Acta Crystallogr., Sect. B* **2005**, *61*, 250−257.
(30) Mathey, Y.; Mercier, H.; Michalowicz, A.; Leblanc, A. *J. Phys. Chem. Solids* **1985**, *46*, 1025−1029.
(31) Mathey, Y.; Michalowicz, A.; Toffoli, P.; Vlaic, G. *Inorg. Chem.* **1984**, *23*, 897−902.